

MEASUREMENT OF THE t -CHANNEL SINGLE TOP-QUARK CROSS SECTIONS WITH THE ATLAS DETECTOR AT THE LHC

K. BECKER on behalf of the ATLAS Collaboration
*Bergische Universität Wuppertal, Gausstr. 20
D-42119 Wuppertal, Germany*

The production of single top quarks at the LHC is dominated by the t -channel exchange of a virtual W boson that is emitted by a light quark inside one of the colliding protons. Thus, the measurement of the top-quark and top-antiquark production cross sections is sensitive to the u -quark and the d -quark parton distribution functions (PDF) and can provide complementary input with respect to other high- p_T processes. Furthermore, the cross section is proportional to the square of the CKM matrix element $|V_{tb}|$ and the measurement can thus provide additional input to constrain the quark mixing matrix without assumptions on the number of quark generations. In this measurement neural networks are used to separate the t -channel signal from the backgrounds after an event selection. Results for t -channel single top-quark production are presented at a center of mass energy of $\sqrt{s} = 7$ TeV and $\sqrt{s} = 8$ TeV using data recorded by the ATLAS detector in 2011 and 2012.

1 Introduction

At the LHC, single top-quark production can occur in three processes. The dominant process, the t -channel exchange of a virtual W boson, has a predicted production cross section of $64.6^{+2.7}_{-2.0}$ pb¹ at a center-of-mass energy of $\sqrt{s} = 7$ TeV and of $87.8^{+3.4}_{-1.9}$ pb¹ at $\sqrt{s} = 8$ TeV. The single top-quark final state provides a direct probe of the Wtb coupling and thus determines V_{tb} without assumptions about the number of quark generations and is sensitive to many models of new physics³. The difference between the top-quark and -antiquark t -channel cross sections is directly related to the difference of the up-quark and the down-quark distribution functions (PDF) of the proton. This report presents measurements of the inclusive cross-sections in the t -channel at $\sqrt{s} = 7$ TeV with 1.0 fb^{-1} ⁴ and at $\sqrt{s} = 8$ TeV with 5.8 fb^{-1} ⁵ of data recorded by the ATLAS detector² in 2011 and 2012. Furthermore measurements of the cross-sections for single top-quark and single top-antiquark production, $\sigma_t(t)$ and $\sigma_t(\bar{t})$, and a measurement of the cross-section ratio $R_t \equiv \sigma_t(t)/\sigma_t(\bar{t})$ ⁶ at $\sqrt{s} = 7$ TeV with 4.7 fb^{-1} of data are presented. The measurements of $\sigma_t(t)$, $\sigma_t(\bar{t})$ and R_t are sensitive to the PDFs of the u -quark and the d -quark in the momentum fraction (x) regime of $0.02 < x < 0.5$.

2 Event selection and background estimation

Top quarks decay almost always into a b quark and a W boson. For the analyses considered here, the single top signal comprises of a leptonically decaying W boson with one or two additional jets. The strategy for all analyses presented is to first reduce the large multijet and W +jets backgrounds to the single top signature with a tight event selection. Lepton candidates, e or μ , are required to be well reconstructed and isolated and to have $p_T > 25$ GeV and $|\eta| < 2.5$. Particle jets are reconstructed using the anti- k_T algorithm with a width parameter of 0.4. Only

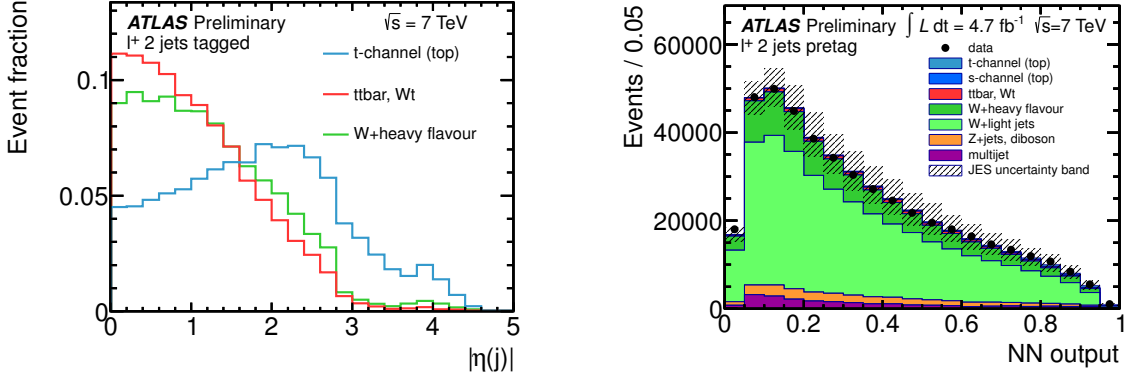


Figure 1: Left: Normalised distribution of the $|\eta(\text{u-jet})|$ variable in the 2-jets tagged l^+ data set. The signal shape is shown together with the shape of the two largest backgrounds. Right: The neural network output in the pretag control region for the $W+2\text{-jet}$ data set with positive lepton charge. The error band in this plot represents the jet energy scale uncertainty on the normalisation. These plots are taken from the $\sqrt{s} = 7$ TeV cross-section ratio analysis⁶.

jets with $p_T > 25$ GeV or $p_T > 30$ GeV in the $\sqrt{s} = 8$ TeV measurement and $|\eta| < 4.5$ are considered. Jets containing bottom quarks are identified (“tagged”) in the region $|\eta| < 2.5$ using a neural network technique. The final event selection requires exactly one charged lepton, e or μ , exactly two jets or exactly three jets where exactly one b -jet is tagged, and missing transverse energy $E_T^{\text{miss}} > 25(30)$ GeV. Further cuts on the the missing transverse energy and the reconstructed mass of the W -boson $m_T(W)$ are applied to reduce the multijet background.

The main backgrounds to the single-top quark final state are QCD multijet events, W boson production in association with jets, and top pair production($t\bar{t}$). Smaller backgrounds originate from Z +jets, Wt -channel and s -channel single-top production, and diboson production. Multijet events contribute as a background to the selected sample if one of the jets in the event is misidentified as an isolated lepton or if the event has a non-prompt lepton that appears isolated. The multijet background is estimated using a data-driven method and performing a binned maximum likelihood fit to the E_T^{miss} distribution. The kinematic distributions for the W +jets background are taken from Monte Carlo samples, while the overall normalisation and the flavour composition are derived from data when extracting the result of the analysis. The $t\bar{t}$ background and other smaller backgrounds are normalised to their theory predictions.

3 Measurement of the t -channel cross sections and R_t

To extract the t -channel signal further from the backgrounds, a neural network technique is used, that combines several variables into one discriminant. The variables with the most discriminating power are the reconstructed top-quark mass $m_{l\nu b}$ and the pseudorapidity of the untagged jet $|\eta(\text{u-jet})|$. For the inclusive cross-section measurements there are two exclusive analysis channels, one with exactly two selected jets and one with exactly three jets in the final state. The R_t analysis is performed in four independent channels: l^+ and l^- for two and three jets. For each analysis channel one neural network is trained and validated in a control region. The discriminating power of the $|\eta(\text{u-jet})|$ variable and an example for the validation plot of a neural network are shown in Figure 1.

The impact of the systematic uncertainties on the measurement affecting the normalisation of the individual backgrounds, the signal acceptance and the shape of the individual predictions, are computed from the results of pseudo-experiments taking into account the correlations between uncertainty sources. The impact of the systematic uncertainties on the measurement is estimated from these pseudo-experiments. In addition, uncertainties on the object modeling, the Monte Carlo generators, the PDFs, the background normalisation to data, and integrated luminosity are

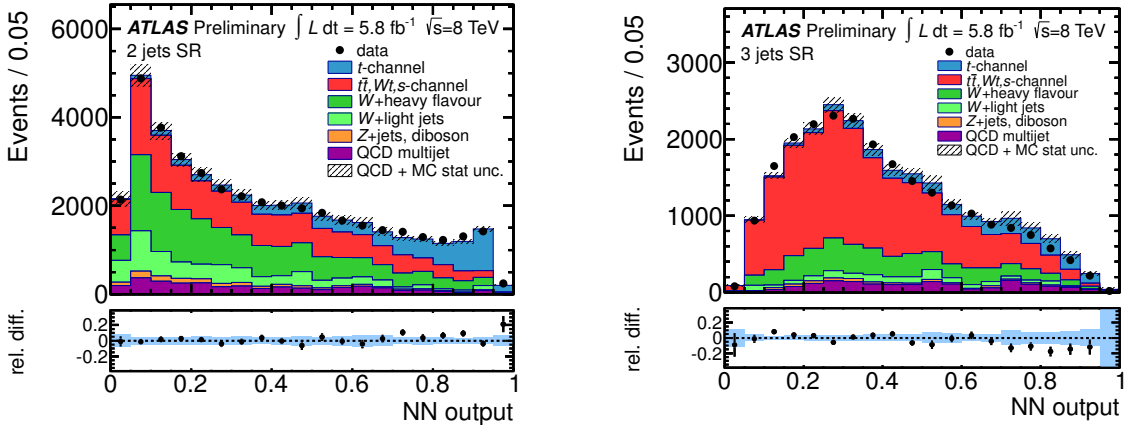


Figure 2: Neural network output distributions for the two-jet (left) and three-jet (right) sample used in the $\sqrt{s} = 8$ TeV cross-section measurements⁵. The signal and backgrounds are normalised to the fit result. The bottom panels show the relative difference between observed data and expectation. The blue shaded band reflects the uncertainty from the limited MC statistics and the uncertainty on the QCD multijet normalisation.

considered in the measurement. The largest systematic effects on the cross section measurements stem from the jet energy scale, the b -tagging efficiency and the uncertainty of initial and final state radiation on the signal.

To extract the signal content of the selected sample, a simultaneous maximum likelihood fit to all NN output distributions used in the analysis is performed. An example for a NN output distribution normalized to the fit values is shown in Fig. 2 for the two and three jets analysis channel.

With the inclusive cross section results the value of $|V_{tb}|$ is extracted by dividing the observed cross section by the standard model expectation¹. The experimental and theoretical uncertainties are added in quadrature. The cross section ratio $R_t \equiv \sigma_t(t)/\sigma_t(\bar{t})$ is calculated using the fit results for the top-quark and the top-antiquark production cross sections. Here the effect of the uncertainties are again estimated with pseudo experiments.

4 Results

Single top quark production in the t -channel has been studied in $\sqrt{s} = 7$ TeV and $\sqrt{s} = 8$ TeV pp collision data recorded with the ATLAS detector in 2011 and 2012. With 1.0 fb^{-1} of $\sqrt{s} = 7$ TeV data the inclusive cross section was measured with the techniques described in this report: the measured t -channel cross section is $\sigma_t(t + \bar{t}) = 83 \pm 20 \text{ pb}$ and the corresponding coupling at the Wtb vertex is $|V_{tb}| = 1.13_{-0.13}^{+0.14}$. In the $\sqrt{s} = 8$ TeV data using 5.8 fb^{-1} and the same analysis technique the t -channel production cross section is measured to $\sigma_t(t + \bar{t}) = 95 \pm 18 \text{ pb}$ corresponding to a coupling of $|V_{tb}| = 1.04_{-0.11}^{+0.10}$. Using the full ATLAS dataset of $\sqrt{s} = 7$ TeV data corresponding to 4.7 fb^{-1} the top-quark and top-antiquark cross sections were measured separately and their ratio was extracted. The measured t -channel single top-quark production cross section is $\sigma_t(t) = 53.2 \pm 1.7$ (stat.) ± 10.6 (syst.) pb, while the top-antiquark production cross section is $\sigma_t(\bar{t}) = 29.5 \pm 1.5$ (stat.) ± 7.3 (syst.) pb. This results into a measured cross-section ratio of $R_t = 1.81 \pm 0.10$ (stat.) $_{-0.20}^{+0.21}$ (syst.). An overview of all cross section results is given in Figure 3, that illustrates the excellent agreement of the results with the standard model predictions. By analyzing the complete $\sqrt{s} = 8$ TeV dataset the single top t -channel production will be studied with a high statistics data sample reaching an improved precision. The measured value of R_t is compared to the predictions obtained with different PDF sets in Figure 3. The graph shows the sensitivity of the result to the parton distribution function and can be used to further improve the understanding of the u- and d-quark PDFs.

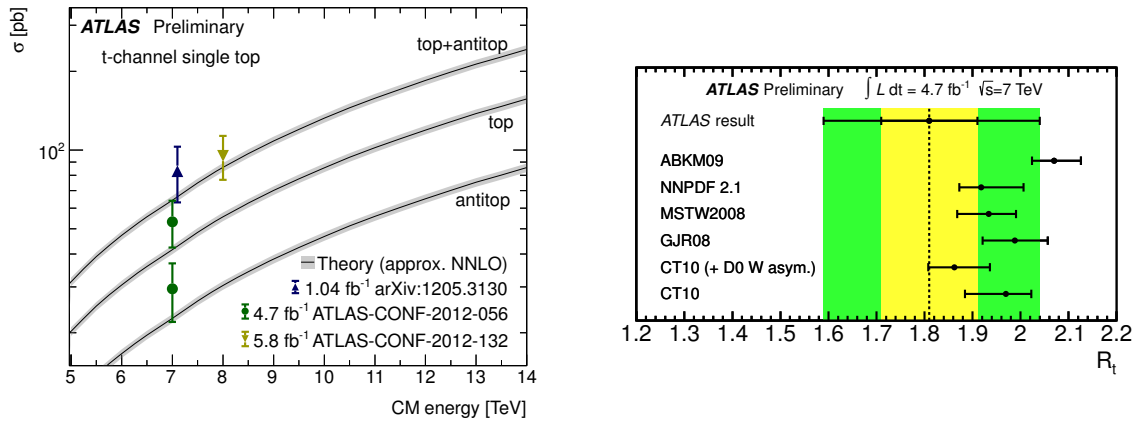


Figure 3: Result for the cross-sections at $\sqrt{s} = 7$ TeV and $\sqrt{s} = 8$ TeV (left)⁵ and for R_t with its statistical (yellow band) and total (green band) uncertainty compared to the calculated values for different NLO PDF sets⁶.

References

1. N. Kidonakis, *Phys. Rev. D* **83**, 091503 (2011).
2. ATLAS Collaboration, 2008 JINST 3 S08003.
3. T. M. Tait and C.-P. Yuan, *Phys. Rev. D* **63**, 014018 (2000).
4. ATLAS Collaboration, *Phys. Lett. B* **717**, 330-350 (2012).
5. ATLAS Collaboration, ATLAS-CONF-2012-132 (2012).
<https://cdsweb.cern.ch/record/1478371>.
6. ATLAS Collaboration, ATLAS-CONF-2012-056 (2012).
<https://cdsweb.cern.ch/record/1453783>.